Small-Molecule Lysophosphatidic Acid Receptor 5 (LPAR5) Antagonists: Versatile Pharmacological Tools to Regulate Inflammatory Signaling in BV-2 Microglia Cells

Ioanna Plastira[1], Lisha Joshi[1], Eva Bernhart[1], Jens Schoene[2], Edgar Specker[2], Marc Nazare[2,3] and Wolfgang Sattler[1,4]*

[1]Gottfried Schatz Research Center, Molecular Biology and Biochemistry, Medical University of Graz, Graz, Austria, [2]Leibniz-Forschungsinstitut für Molekulare Pharmakologie (FMP), Berlin, Germany, [3]Berlin Institute of Health (BIH), Charite & MDC, Berlin, Germany, [4]Center for Explorative Lipidomics, BioTechMed-Graz, Graz, Austria

Lysophosphatidic acid (LPA) species in the extracellular environment induce downstream signaling *via* six different G protein-coupled receptors (LPAR1–6). These signaling cascades are essential for normal brain development and function of the nervous system. However, in response to acute or chronic central nervous system (CNS) damage, LPA levels increase and aberrant signaling events can counteract brain function. Under neuro-inflammatory conditions signaling along the LPA/LPAR5 axis induces a potentially neurotoxic microglia phenotype indicating the need for new pharmacological intervention strategies. Therefore, we compared the effects of two novel small-molecule LPAR5 antagonists on LPA-induced polarization parameters of the BV-2 microglia cell line. AS2717638 is a selective piperidine-based LPAR5 antagonist (IC_{50} 0.038 µM) while compound 3 is a diphenylpyrazole derivative with an IC_{50} concentration of 0.7 µM in BV-2 cells. Both antagonists compromised cell viability, however, at concentrations above their IC_{50} concentrations. Both inhibitors blunted LPA-induced phosphorylation of STAT1 and STAT3, p65, and c-Jun and consequently reduced the secretion of pro-inflammatory cyto-/chemokines (IL-6, TNFα, IL-1β, CXCL10, CXCL2, and CCL5) at non-toxic concentrations. Both compounds modulated the expression of intracellular (COX-2 and Arg1) and plasma membrane-located (CD40, CD86, and CD206) polarization markers yet only AS2717638 attenuated the neurotoxic potential of LPA-activated BV-2 cell-conditioned medium towards CATH.a neurons. Our findings from the present *in vitro* study suggest that the two LPAR5 antagonists represent valuable pharmacological tools to interfere with LPA-induced pro-inflammatory signaling cascades in microglia.

Keywords: LPA5, microglia, chemokines, cytokines, neurotoxicity, transcription factors

INTRODUCTION

The brain is an immune-privileged organ (Ransohoff and Brown, 2012), yet the central nervous system (CNS) is able to mount a primary immune response since host defense mechanisms are operative in astrocytes and microglia. Microglia are the resident immune cells of CNS and able to detect subtle alterations of the finely tuned micromilieu in the CNS (Ransohoff and Perry, 2009; Ransohoff and Cardona, 2010; Garaschuk and Verkhratsky, 2019; Norris and Kipnis, 2019). Microglia cover the whole CNS parenchyma and originate from embryonic progenitors in the yolk sac (Ginhoux et al., 2010; Butovsky and Weiner, 2018). These cells are unevenly distributed in the brain acquiring different morphologies, ranging from small, round cells to those having multiple branched processes (Hammond et al., 2018). These cells are a self-renewing, long-lived *in vivo* population, not replaced by peripheral monocytes (Ginhoux and Prinz, 2015), with a critical role in both, the physiological and pathological brain (Salter and Stevens, 2017; Hammond et al., 2018; Smolders et al., 2019). In their "resting" state, microglia processes scan their environment and respond to danger signals (Nimmerjahn et al., 2005). They are equipped with a unique cluster of transcripts encoding proteins for sensing endogenous ligands, collectively termed the microglia *sensome* (Hickman et al., 2013).

Within the last years, great progress in understanding and analyzing differences in microglia responses under pathological conditions has been made (Colonna and Butovsky, 2017; Wolf et al., 2017). Microglia regulate numerous aspects of inflammation, such as regeneration, cytotoxicity, and immunosuppression depending on their different activation states (Du et al., 2016). During disease progression they appear to be highly heterogeneous in terms of neurotoxic/pro-inflammatory or neuroprotective/anti-inflammatory responses (Tang and Le, 2016). Distinct molecular signatures and different microglia sub-populations have been identified, revealing major spatial, temporal and gender differences (Grabert et al., 2016; Guneykaya et al., 2018; Masuda et al., 2019), as well as differences associated with aging and context of the neurodegenerative disease (Colonna and Butovsky, 2017; Hickman et al., 2018; Song and Colonna, 2018; Mukherjee et al., 2019). Recently, the application of powerful methodologies has revealed unique phenotypic signatures under both physiological and neurodegenerative settings (Tay et al., 2018; Böttcher et al., 2019; Hammond et al., 2019; Masuda et al., 2019).

The lysophosphatidic acid (LPA) family consists of small alkyl- or acyl-glycerophospholipids (molecular mass: 430–480 Da) that act as extracellular signaling molecules through at least six G protein-coupled receptors (GPCRs; Yung et al., 2014). There is a range of structurally related LPA species present in various biological systems (Aoki, 2004). An important aspect of LPA receptor biology is that different LPA species may activate different LPA receptor isoforms (Kano et al., 2008). There are two major synthetic pathways for LPA (Yung et al., 2014). In the first pathway, phospholipids (PLs) are converted to their corresponding lysophospholipids such as lyso-phosphatidylcholine, -serine, or -ethanolamine. This occurs *via* phosphatidylserine-specific phospholipase A1 (PS-PLA1) or

secretory phospholipase A2 (sPLA2) activity. Lysophospholipids are then converted to LPA *via* head group hydrolysis by autotaxin (ATX). In a second synthetic route, phosphatidic acid (PA), produced from PLs through phospholipase D (PLD) activity or from diacylglycerol (DAG) through diacylglycerol kinase (DGK) activity, is subsequently converted to LPA by the actions of either PLA1 or PLA2 (Aoki et al., 2008). LPA acts through specific G protein-coupled LPA receptors (LPAR1-LPAR6) that mediate the diverse effects of these lysophospholipids (Yung et al., 2014).

Under physiological conditions, LPA-mediated signaling is essential for normal neurogenesis and function of the CNS. However, in response to injury LPA levels can increase in brain and CSF (Tigyi et al., 1995; Savaskan et al., 2007; Ma et al., 2010; Yung et al., 2011; Santos-Nogueira et al., 2015). Aberrant LPA signaling contributes to multiple disease states, including neuropathic pain, neurodegenerative, neurodevelopmental and neuropsychiatric disorders, cardiovascular disease, bone disorders, fibrosis, cancer, infertility, and obesity (Yung et al., 2014). Microglia express LPA receptors and are activated by LPA (Möller et al., 2001; Bernhart et al., 2010). In the murine BV-2 microglia cells, LPA activates Ca^{2+}-dependent K^+ currents resulting in membrane hyperpolarization (Schilling et al., 2002) and induces cell migration *via* Ca^{2+}-activated K^+ channels (Schilling et al., 2004). In addition, LPA controls microglial activation and energy homeostasis (Bernhart et al., 2010), modulates the oxidative stress response (Awada et al., 2012), regulates the induction of chronic pain (Sun et al., 2012), and interferes with pro-inflammatory cytokine production (Awada et al., 2014).

LPAR5 was identified through screening approaches directed towards the deorphanization of GPR92 (Kotarsky et al., 2006). Signaling through the $G_{12/13}$ pathway induces neurite retraction, stress fiber formation, and receptor internalization *in vitro*, while activation of G_q increases intracellular calcium levels and induce cAMP accumulation (Lee et al., 2006). LPAR5 is expressed in various tissues both in humans and mice (Amisten et al., 2008; Lundequist and Boyce, 2011; Yung et al., 2014). In the CNS, LPAR5 was found in the early embryonic forebrain, midbrain, and hindbrain of Slc:ddY mice. This expression pattern becomes more ubiquitous from E9.5–E12.5, showing diffuse patterns in the developing brain and choroid plexus revealing a role for LPAR5 in brain development (Ohuchi et al., 2008). LPAR5 signaling contributes to nerve injury-triggered pain (Lin et al., 2012; Ueda et al., 2013) and multiple sclerosis-associated neuropathic pain (Tsukahara et al., 2018). Findings that LPAR5 is activated during nerve injury (but not under basal conditions) are consistent with the fact that LPA levels rise significantly in response to spinal cord injury (Ma et al., 2010; Santos-Nogueira et al., 2015). Activated microglia were also suggested to contribute to demyelination in the injured spinal cord (Santos-Nogueira et al., 2015).

Although LPAR5 signaling was mainly studied in the context of neuropathic pain, we could recently show that LPAR5 affects microglia biology and induces a distinct pro-inflammatory and migratory signature (Plastira et al., 2016, 2017). The identification of the LPA/LPAR5 axis as a signaling pathway

contributing to the inflammatory response of microglia might foster deeper insights into LPA-mediated effects on the resident immune cells of the brain. Since the binding domain of LPAR5 represents an extracellular target, it is ideally suited for pharmacological intervention. Accordingly, LPAR5 specific antagonists were developed to modulate the LPA/LPAR5 axis and study its role in development and progression of (neuro-) inflammatory diseases (Kozian et al., 2012, 2016; Murai et al., 2017; Kawamoto et al., 2018). In the present study, we analyzed the potential of two structurally diverse non-lipid LPAR5 antagonists (compound 3 and AS2717638; Kozian et al., 2016; Murai et al., 2017) to interfere with LPA-induced inflammatory signaling cascades in BV-2 microglia cells.

MATERIALS AND METHODS

Materials
Cell culture medium RPMI1640, fetal calf serum (FCS), antibiotics, culture reagents, and trypsin were from Invitrogen (Waltham, MA, USA). LPA (1-oleoyl-2-hydroxy-sn-glycero-3-phosphate; LPA18:1) was from Sigma-Aldrich (St. Louis, MO, USA). Antibodies against COX-2, Arginase-1 and the nonphosphorylated and phosphorylated p65-NFkB, c-Jun, STAT1, and STAT3 were from Cell Signaling (Beverly, MA, USA); PE-CD40, APC-CD86, PE-CD206 antibodies and their isotype controls were from Biolegend (San Diego, CA, USA). Monoclonal anti-mouse β-actin (clone AC-74) was from Sigma-Aldrich (St. Louis, MO, USA). The LPAR5 inhibitors, AS2717638 [6,7-Dimethoxy-2-(5-methyl-1,2-benzoxazol-3-yl)-4-(piperidin-1-ylcarbonyl)isoquinolin-1(2H)-one] and compound 3 [4-((2-((1-(2,4-dichlorophenyl)-4-methyl-5-(4-(trifluoromethyl)phenyl)-1H-spyrazol-3-yl)methoxy)-2-methylpropanamido)methyl)benzoic acid] were synthesized according to the published procedures (Kozian et al., 2016; Murai et al., 2017).

For AS2717638, mass analysis was performed with an Agilent Technologies 6230 Accurate Mass TOF LC/MS linked to Agilent Technologies HPLC 1260 Series using a Thermo Accuore RP-MS column (30 × 2.1 mm, 2.6 μm particle size; Eluent A: H_2O with 0.1% formic acid Eluent B: MeCN with 0.1% formic acid; Gradient: 0.00 min 95% A, 0.2 min 95% A, 1.1 min 1% A, 2.5 min stop-time, 1.3 min post-time; Flow rate: 0.8 ml/min; UV-detection: 220 nm, 254 nm, and 300 nm). LC-MS: R_t = 1.873 min; HRMS (ESIpos): m/z [M + H]$^+$ experimentally determined = 448.1454, calculated for $C_{25}H_{25}N_3O_5$ = 448.1467.

^{1}H NMR (300 MHz, DMSO-d_6) δ 7.80–7.75 (m, 2H), 7.64 (s, 1H), 7.62–7.56 (m, 2H), 6.95 (s, 1H), 3.94 (s, 3H), 3.93 (s, 3H), 3.75–3.52 (m, 2H), 3.52–3.36 (m, 2H), 2.44 (s, 3H), 1.68–1.54 (m, 4H), 1.54–1.43 (m, 2H). ^{13}C NMR (75 MHz, DMSO) δ 164.7, 163.1, 159.5, 156.8, 154.6, 150.1, 134.3, 133.2, 130.0, 128.8, 122.9, 119.2, 117.7, 115.3, 110.6, 108.6, 105.2, 56.4, 56.3, 26.8, 24.4, 21.0.

SwissADME[1] was used for drawing, chemical structure property prediction, and calculations (Daina et al., 2017).

---

[1]http://www.swissadme.ch/

BV-2 Microglia Culture
The murine microglial cell line BV-2 was from Banca Biologica e Cell Factory (Genova, Italy). Cells were cultivated and maintained in RPMI1640 medium supplemented with 10% FCS, 100 U/ml penicillin, 100 mg/ml streptomycin, and 5 ml L-glutamine (200 mM) at 37°C in a humidified incubator under 5% CO_2 and 95% air. When cells reached confluency, they were split into new flasks or they were plated accordingly for the experiments as described previously (Plastira et al., 2016).

CATH.a Neurons Culture
The murine neuronal cell line CATH.a was from ATCC. Cells were grown and maintained in RPMI1640 medium supplemented with 10% horse serum, 5% FCS, 1% penicillin-streptomycin, 0.4% HEPES, and 0.2% sodium pyruvate at 37°C (5% CO_2). When cells reached confluency, they were split into new flasks (subcultivation ratio of 1:4) using 0.12% trypsin without EDTA as described (Waltl et al., 2013).

LPA Treatment
Cells were plated in 6 or 12-well plates and allowed to adhere for 2 days. Cells were always kept in serum-free medium overnight before incubation with LPA and LPA plus each inhibitor. Aqueous LPA stock solutions (5 mM) were stored at −70 °C. Only freshly thawed stocks were used for the experiments.

Inhibitor Treatments
AS2717638 and compound 3 were diluted in DMSO (stock concentration: 10 mM) and kept at −20°C. During the experiments, AS2717638 and compound 3 were used at a final concentration of 0.1 μM and 1 μM, respectively. The highest DMSO concentration was 0.01% (v/v) and used as vehicle control throughout the study.

MTT Assay
The toxicity of the two inhibitors on BV-2 cells was assessed using the MTT assay. Cells were plated in 24-well plates and grown to confluency. The cells were incubated with MTT (1.2 mM; in serum-free medium) for 1 h, washed with PBS and cell lysis was performed with isopropanol/1 M HCl (25:1 v/v) on a rotary shaker at 1,200 rpm for 10 min. Finally the samples were diluted 1:5 and absorbance was measured at 570/650 nm on a Victor 1,420 multilabel counter (Wallac).

Immunoblotting
After treatment with the experimental substances for the indicated time periods, BV-2 cells were washed twice with ice-cold PBS and lysed in RIPA buffer (50 mM Tris-HCl pH 7.4, 1% NP-40, 150 mM NaCl, 1 mM Na_3VO_4, 1 mM NaF, 1 mM EDTA) containing protease inhibitors (Sigma; aprotinin, leupeptin, pepstatin: 1 μg/ml each), 10 μM PMSF and phosphatase inhibitors cocktail (Thermo Scientific, Waltham, MA, USA). Protein content was determined using the BCA kit (Thermo Scientific) and BSA as standard. Protein samples (100 μg) were separated on 10% SDS-PAGE gels and transferred to polyvinylidene difluoride membranes. Membranes were blocked with 5% low-fat milk in Tris-buffered saline containing Tween 20 (TBST) for 2 h at RT and incubated with the primary

antibodies overnight with gentle shaking at 4°C. After the removal of primary antibodies, the membranes were washed for 30 min in TBST and incubated for 2 h at RT with anti-rabbit (1:10,000) or anti-mouse (1:5,000) as secondary antibodies. Following three washes with TBST for 1 h, immunoreactive bands were visualized using ECL or ECL plus reagents and detected with a chemiluminescence detection system (ChemiDoc Bio-Rad, Berkeley, CA, USA). In some cases, the membranes were stripped using a stripping buffer (140 µl β-mercaptoethanol in 20 ml buffer 60 mM Tris/ 2% SDS, pH 6.8) under gentle shaking for 30 min at 50°C in a water bath, washed for 1 h in TBST, blocked with 5% low-fat milk in TBST for 1 h at room temperature and probed with the pan antibodies for p65-NF-kB, c-Jun, STAT1, and STAT3 as described (Plastira et al., 2017). Anti-β-actin (1:5,000) was used as loading controls.

Flow Cytometry

Flow cytometry was used to quantitate the percentage of CD40, CD86, and CD206 positive microglia cells. BV-2 cells were seeded in triplicate onto 6-well at a density of 1×10^5 cells per well. After 24 h serum-starvation, cells were incubated with vehicle control, LPA or LPA plus the antagonists for 12 and 24 h. Cells were then collected, blocked using the Ultra V blocker (Thermo Scientific) and incubated with PE anti-CD40, APC anti-CD86, or PE anti-CD206 antibody (1:50). After fixation, samples were measured using a Guava easyCyte 8 Millipore flow cytometer.

ELISA

IL-1β, TNFα, IL-6, CCL5 (RANTES), CXCL2 (MIP-2), and CXCL10 (IP-10) concentrations in the cellular supernatants were quantitated using the murine ELISA development kits (Peprotech, NJ, USA; Plastira et al., 2016). Briefly, BV-2 cells were seeded in triplicate onto 12-well plates at a density of 5×10^4 cells per well, serum-starved (o/n), and incubated in serum-free medium, containing LPA in the absence or presence of the antagonists for the indicated time periods. For each time point, the supernatants were collected and kept at −70°C until further use. The concentrations of the cytokines and chemokines were determined using the external standard curve.

LDH Assay

Lactate dehydrogenase is a soluble enzyme located in the cytosol and released into the culture medium upon cell lysis or damage. LDH activity can, therefore, be used as an indicator of membrane integrity and thus a measurement of cytotoxicity (Cayman Chemical, Ann Arbor, MI, USA). The assay was performed as previously described (Plastira et al., 2016). In brief, BV-2 cells were seeded in triplicate into 6-well plates at a density of 1×10^5 cells per well, serum-starved overnight and incubated in serum-free medium, containing LPA in the absence or presence of the antagonists for the indicated time periods. For each time point, the supernatants were collected and kept at −70°C until further use.

CATH.a neurons were seeded in a 96-well plate at a concentration of 1×10^5 cells per well, and following overnight serum-starvation, the cells were incubated in the presence of the above-mentioned supernatants. Three wells containing only medium without cells were used for background control. In order to measure maximum and spontaneous release, cells were incubated with 10% Triton X-100 and assay buffer, respectively. After 24 h, the plate was centrifuged at 1,300 rpm for 5 min. One-hundred microliter of the supernatants was transferred to a new 96-well plate and 100 µl of LDH reaction solution was added to each well. The plate was incubated at 37°C for 30 min and the absorbance at 490 nm was measured using a plate reader (Plastira et al., 2017).

Statistical Analysis

All experiments were performed using three replicates per experimental group and repeated three times (unless otherwise stated). Statistical analyses were performed using the GraphPad Prism version 6 for Mac (GraphPad Software, Inc., San Diego, CA, USA). Data obtained from independent measurements were analyzed by one-way ANOVA followed by Bonferroni's *post hoc* test and presented as mean ± SD.

RESULTS

AS2717638 and Compound 3 Inhibit LPA-Mediated Pro-inflammatory Transcription Factor Phosphorylation

Structures and physicochemical properties of AS2717638 and compound 3 are displayed in **Figures 1A,C**. As a first step in our study, we analyzed whether the two LPAR5 antagonists exhibit toxic effects in BV-2 microglia cells. Incubation with increasing concentrations of AS2717638 (0.1–10 µM) revealed that BV-2 cell viability was reduced between 10% and 30% after a 2 h incubation at concentrations ≥0.5 µM (**Figure 1B**). Therefore AS2717638 was used at 0.1 µM in all experiments. After a 24 h incubation, cell viability was decreased by 55 and 70% (1 and 10 µM, respectively; **Figure 1B**). In contrast, compound 3 reduced viability by 50 (2 h) and 60 (24 h) % only at the highest concentration (10 µM) used (**Figure 1D**). In the experiments described below, compound 3 was used at 1 µM, a concentration without detrimental effects on cell viability. At these concentrations, both inhibitors attenuated LPA-mediated morphological changes (cell perimeter and cellular surface area) of BV-2 cells (**Supplementary Figure S1**).

During previous experiments, we examined the effect of LPA on microglial inflammatory response and reported that LPAR5 controls the LPA induced pro-inflammatory phenotype in microglia cells (Plastira et al., 2017). In order to test the impact of AS2717638 and compound 3 on activation/phosphorylation of transcription factors in BV-2 cells in response to LPA (1 µM) treatment, we used immunoblot analysis. Cells were incubated in the presence or absence of each inhibitor for different time periods and the activation of transcription factors was analyzed. Results of these experiments indicated that both LPAR5 antagonists clearly suppressed LPA-induced phosphorylation of p65-NF-kB, c-Jun, STAT1, and STAT3 (**Figure 2**). AS2717638 used at 0.1 µM attenuated STAT1 and STAT3 phosphorylation back to or below baseline at the 8 h time point, and comparable results were obtained for pp65 and pcJun (**Figure 2A**). Also compound 3 (1 µM) decreased phosphorylation of all transcription factors at one or more time
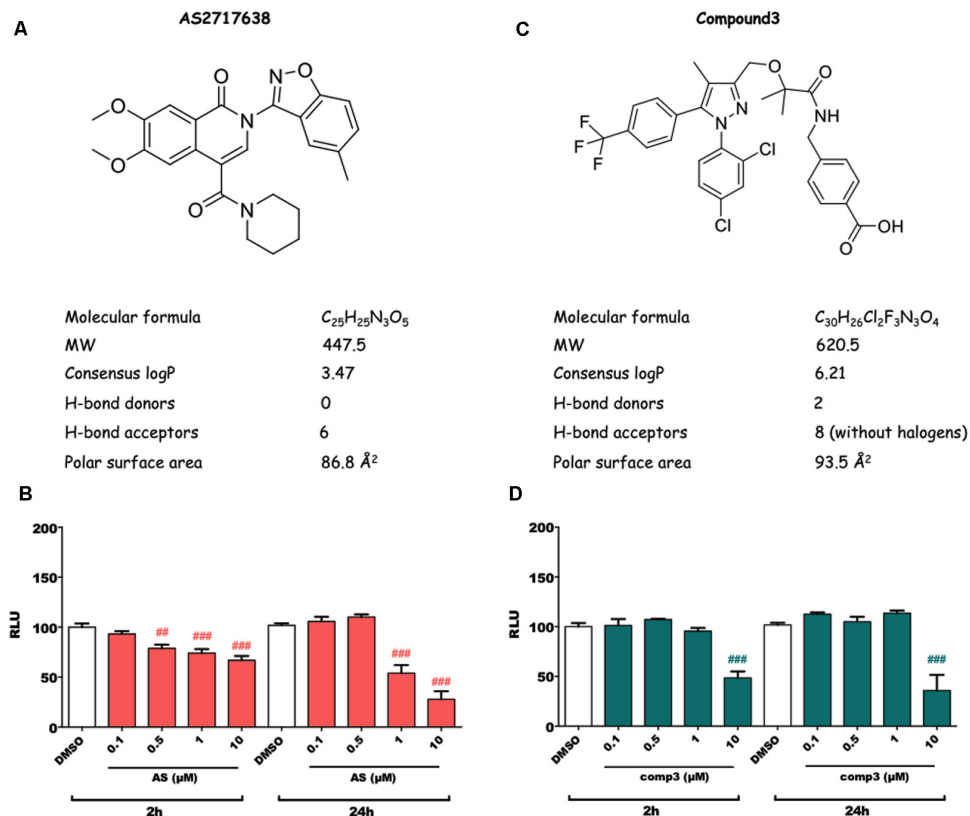
FIGURE 1 | Structure, physicochemical properties and cytotoxic potential of AS2717638 and compound 3. Chemical structures of AS2717638 **(A)** and compound 3 **(C)**. SwissADME was used to calculate physicochemical properties relevant to the "*rule of five*" that predict drug-likeness of a compound (Lipinski et al., 2001). Cytotoxicity was assessed using the MTT assay. BV-2 microglia cells were cultured in 6-well plates, serum-starved overnight (o/n) and incubated with the indicated concentrations of AS2717638 **(B)** and compound 3 **(D)** in DMSO for 2 and 24 h. DMSO was used as vehicle control. For convenience, the names of the inhibitors are presented as AS and comp3. Results from three independent experiments in triplicates are presented as mean ± SD ($^{##}p < 0.01$, $^{###}p < 0.001$ compared to vehicle control; one-way ANOVA with Bonferroni correction).

points (**Figure 2B**). The bar graphs represent densitometric analysis from three independent experiments.

AS2717638 and Compound 3 Attenuate LPA-Induced Cyto-/Chemokine Secretion by BV-2 Microglia

We then quantitated the concentrations of secreted IL-6, TNFα, IL-1β, CXCL10, CXCL2, and CCL5 using ELISA kits (**Figure 3**). These experiments revealed that both, AS2717638 and compound 3 decreased secretion of IL-6, TNFα, IL-1β, CXCL10, CXCL2, and CCL5 almost back to base-line levels. For AS2717683 the decrease in CXCL2 concentrations was statistically not significant.

LPA-Induced Pro-inflammatory Marker Expression Is Attenuated by AS2717638 and Compound 3

In the next set of experiments, we analyzed the impact of LPAR5 antagonism on the expression of pro- and anti-inflammatory markers using Western blotting and flow cytometry. Immunoblotting experiments revealed that treatment

with AS2717638 (**Figure 4A**) or compound 3 (**Figure 4C**) significantly reduced LPA-dependent COX-2 expression yet only AS2717638 could increase the expression of Arg-1, a marker protein for the M2 microglia/macrophage phenotype. Densitometric evaluation of immunoreactive bands from three separate experiments is given in the bar graphs (**Figures 4B,D**). Using flow cytometry, we then analyzed the expression pattern of specific polarization surface markers in LPA-stimulated BV-2 cells in the absence or presence of the antagonists. As shown in **Figures 4E,F**, both antagonists abrogated LPA-mediated CD40 and CD86 (except AS2717638 at 24 h) upregulation, whereas CD206 levels were only upregulated by AS2717638 (**Figure 4G**). Scatterplots representative of these analyses are shown in **Supplementary Figure S2**.

AS2717638, but Not Compound 3, Reduces Neurotoxic Properties of Conditioned Medium Collected From LPA-Stimulated BV-2 Cells
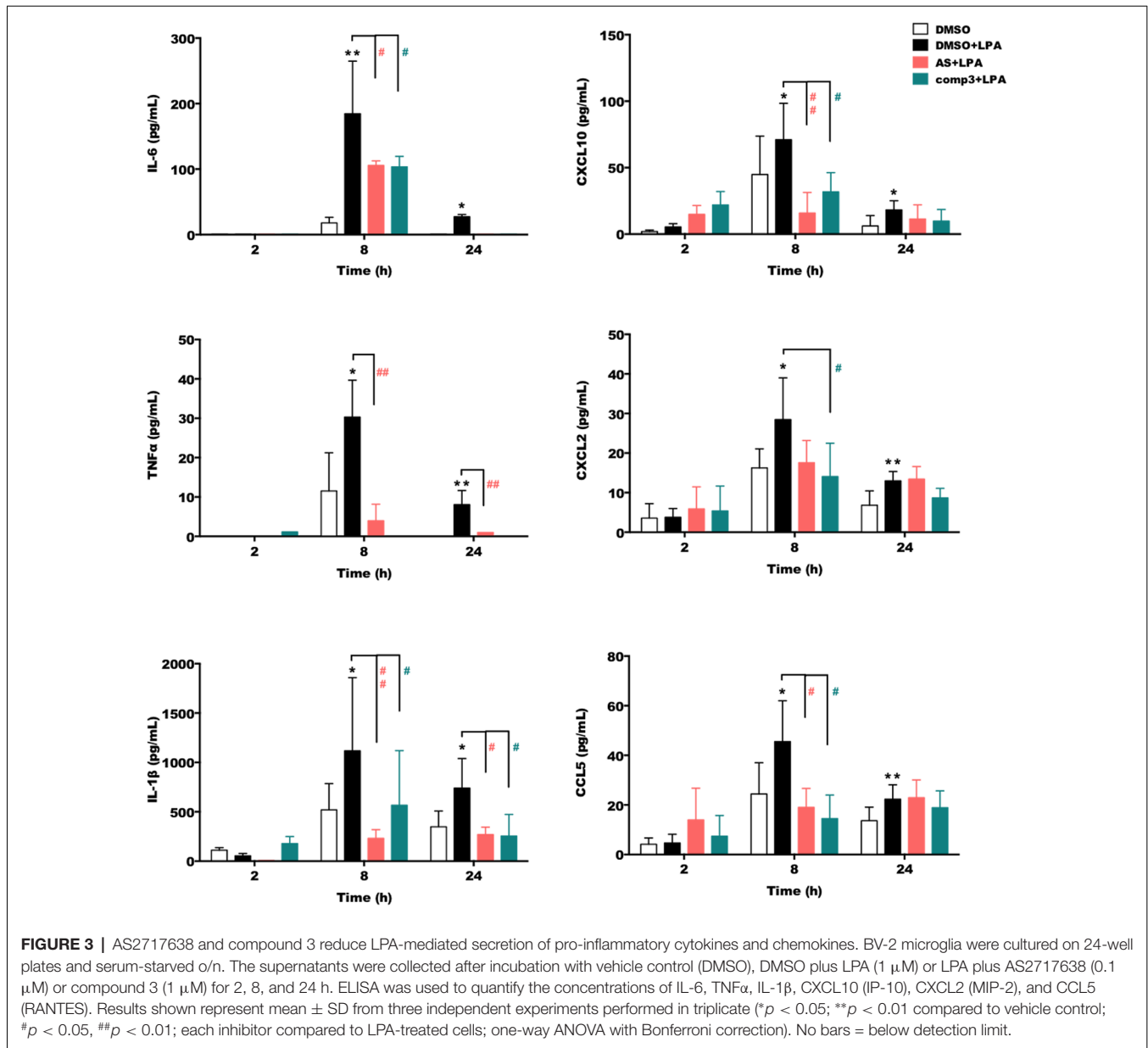
CATH.a neurons were incubated with the supernatants collected from LPA-treated (in the absence or presence of AS2717638 or
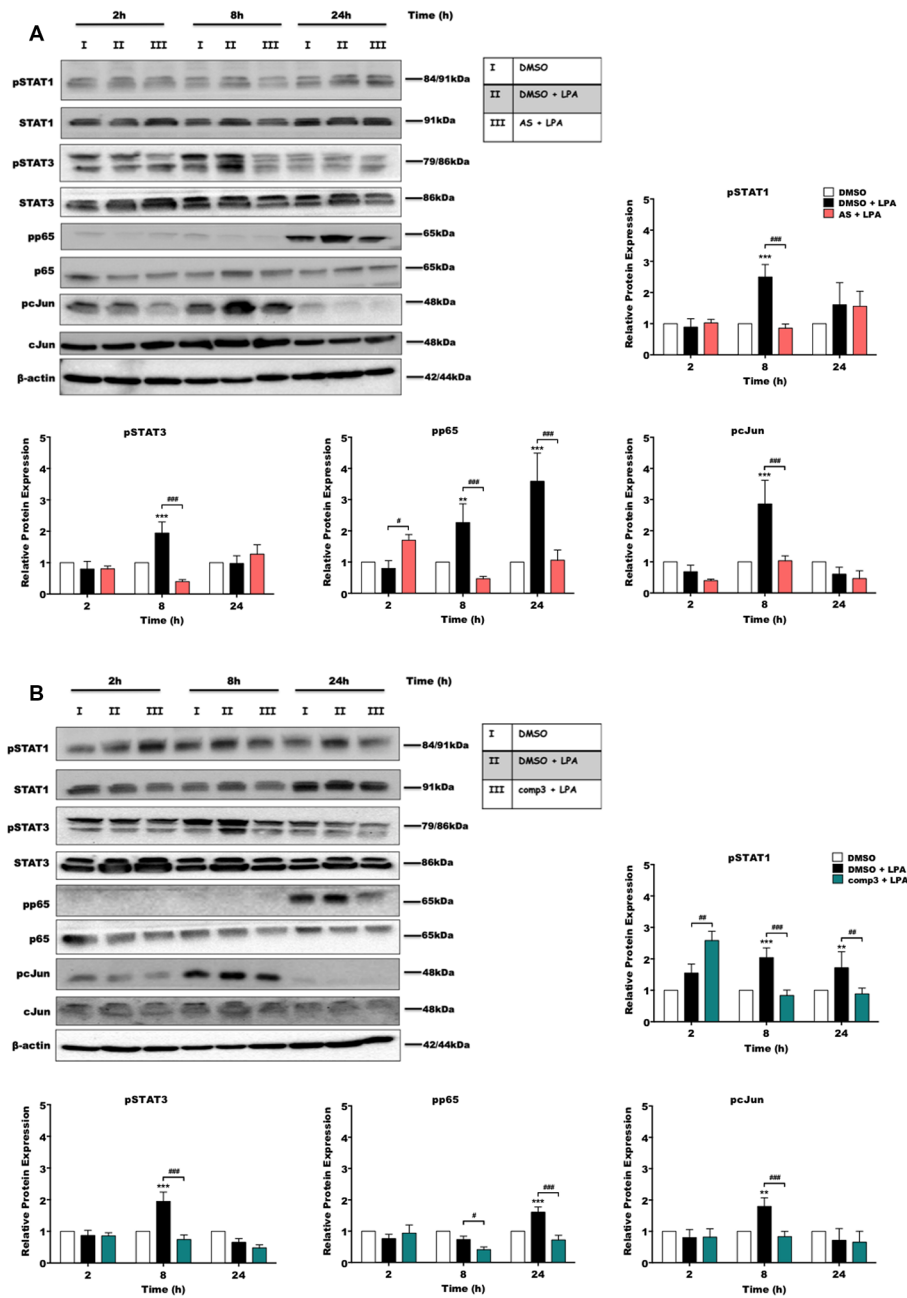
FIGURE 2 | AS2717638 and compound 3 attenuate lysophosphatidic acid (LPA)-induced phosphorylation of pro-inflammatory transcription factors. BV-2 microglia cells were cultured in 6-well plates and serum-starved o/n. Cells were treated with DMSO, DMSO plus LPA (1 μM), and LPA (1 μM) in the presence of **(A)** AS2717638 (0.1 μM) or **(B)** compound 3 (1 μM) for the indicated time periods and cell protein lysates were collected. The phosphorylation states along with the total levels of STAT1, STAT3, p65-NF-kB, and c-Jun were detected using Western blotting. If two bands appeared for one protein [e.g., (p)STAT3] both bands were included in the densitometric evaluation. Protein/loading control ratios were normalized to the ratio of unstimulated microglia (mean value of DMSO controls was set to 1). One representative blot out of three separate experiments and the densitometric analysis of each protein expression from three independent experiments is presented (**$p < 0.01$; ***$p < 0.001$ compared to DMSO-treated cells; #$p < 0.05$; ##$p < 0.01$; ###$p < 0.001$ each inhibitor compared to LPA-treated cells; one-way ANOVA with Bonferroni correction).

compound 3) BV-2 cells. Neuronal cell death was quantified using an LDH activity kit (Plastira et al., 2017). BV-2 medium collected from LPA-stimulated cells induced a 2.5-fold increase in LDH activity in CATH.a cultures (**Figure 4H**, gray bars).

In contrast, medium collected from LPA-activated microglia that were cultured in the presence of AS2717638 did not affect neuronal viability (red bars). Although compound 3 showed a tendency to decrease cytotoxic effects of microglia-conditioned

FIGURE 3 | AS2717638 and compound 3 reduce LPA-mediated secretion of pro-inflammatory cytokines and chemokines. BV-2 microglia were cultured on 24-well plates and serum-starved o/n. The supernatants were collected after incubation with vehicle control (DMSO), DMSO plus LPA (1 μM) or LPA plus AS2717638 (0.1 μM) or compound 3 (1 μM) for 2, 8, and 24 h. ELISA was used to quantify the concentrations of IL-6, TNFα, IL-1β, CXCL10 (IP-10), CXCL2 (MIP-2), and CCL5 (RANTES). Results shown represent mean ± SD from three independent experiments performed in triplicate (*$p < 0.05$; **$p < 0.01$ compared to vehicle control; #$p < 0.05$, ##$p < 0.01$; each inhibitor compared to LPA-treated cells; one-way ANOVA with Bonferroni correction). No bars = below detection limit.

medium these effects were statistically not significant (**Figure 4H**, green bars).
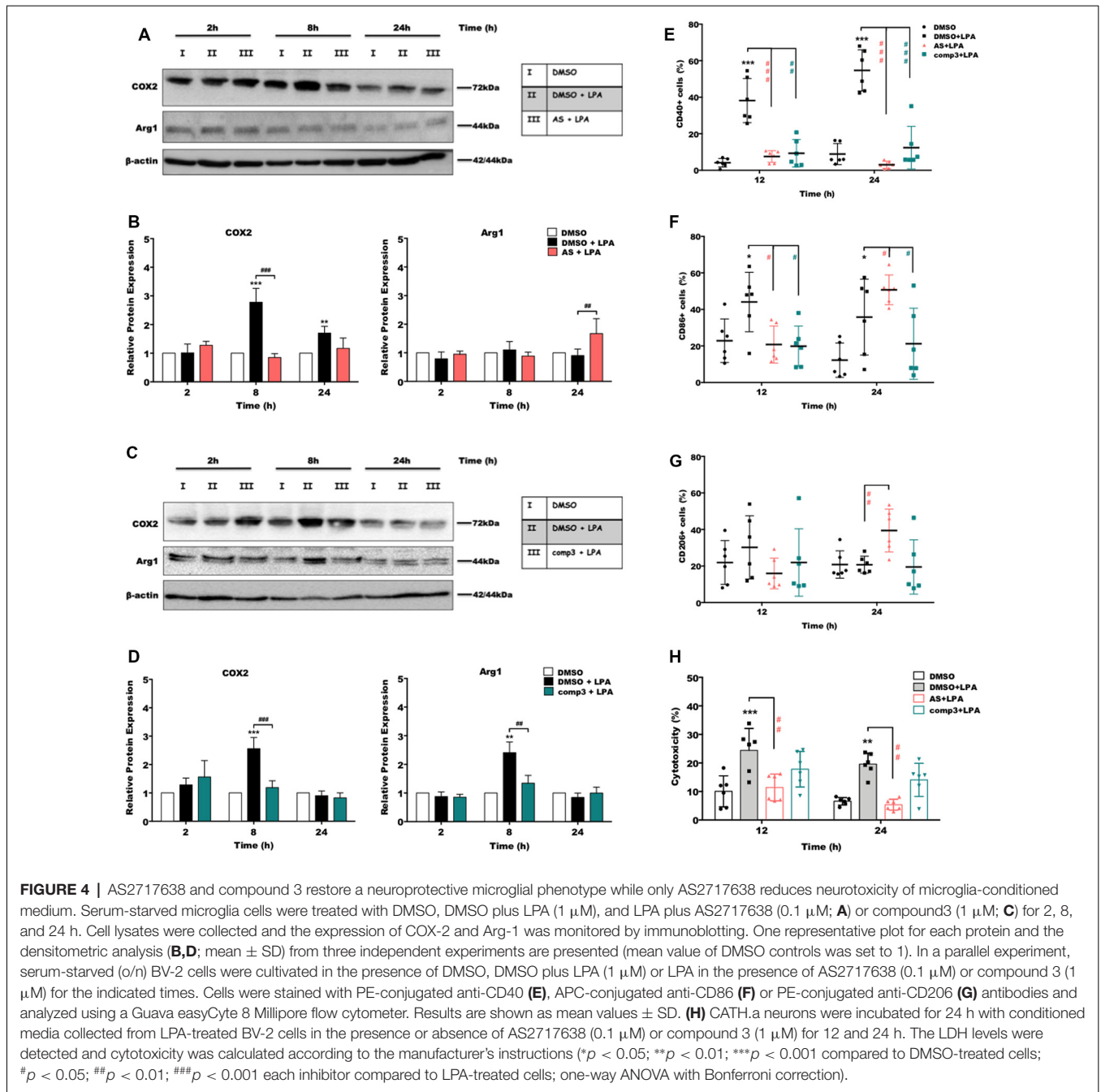
DISCUSSION

Depending on the disease context, extrinsic signals determine whether microglia acquire a beneficial or detrimental phenotype. Their critical role in CNS homeostasis makes these cells potential therapeutic targets, which necessitate a thorough understanding of different phenotypic subclasses, transcriptome profiles, and pathways that modulate their function.

In numerous pathological conditions, such as (neuro-) inflammation, brain injury, neuropathic pain and gliomas, LPA levels can increase and through downstream signaling counteract brain function. Aberrant ATX-LPA signaling has

been implicated in several neurological disorders including neuropathic pain and schizophrenia (Yang et al., 2015). LPA levels were elevated in a controlled cortical impact mouse model of TBI (Crack et al., 2014; Eisenried et al., 2017), in Huntington's disease mouse brains (Vodicka et al., 2015) and in glioblastoma multiforme (Tabuchi, 2015). Tissue distribution analyses revealed that ATX gene expression is induced in human AD frontal cortex and the TauP301L mouse model (Umemura et al., 2006). Altered expression levels and activity of ATX with accompanying alterations in LPA signaling have recently been implicated in the pathogenesis of AD (Ramesh et al., 2018).

Due to its importance in numerous diseases, ATX makes an attractive target for therapeutic intervention (Matralis et al., 2019). However, there may be therapeutic benefit by selectively targeting one or more LPA receptor subtypes (Herr et al.,

FIGURE 4 | AS2717638 and compound 3 restore a neuroprotective microglial phenotype while only AS2717638 reduces neurotoxicity of microglia-conditioned medium. Serum-starved microglia cells were treated with DMSO, DMSO plus LPA (1 μM), and LPA plus AS2717638 (0.1 μM; **A**) or compound3 (1 μM; **C**) for 2, 8, and 24 h. Cell lysates were collected and the expression of COX-2 and Arg-1 was monitored by immunoblotting. One representative plot for each protein and the densitometric analysis (**B,D**; mean ± SD) from three independent experiments are presented (mean value of DMSO controls was set to 1). In a parallel experiment, serum-starved (o/n) BV-2 cells were cultivated in the presence of DMSO, DMSO plus LPA (1 μM) or LPA in the presence of AS2717638 (0.1 μM) or compound 3 (1 μM) for the indicated times. Cells were stained with PE-conjugated anti-CD40 (**E**), APC-conjugated anti-CD86 (**F**) or PE-conjugated anti-CD206 (**G**) antibodies and analyzed using a Guava easyCyte 8 Millipore flow cytometer. Results are shown as mean values ± SD. (**H**) CATH.a neurons were incubated for 24 h with conditioned media collected from LPA-treated BV-2 cells in the presence or absence of AS2717638 (0.1 μM) or compound 3 (1 μM) for 12 and 24 h. The LDH levels were detected and cytotoxicity was calculated according to the manufacturer's instructions (*$p < 0.05$; **$p < 0.01$; ***$p < 0.001$ compared to DMSO-treated cells; #$p < 0.05$; ##$p < 0.01$; ###$p < 0.001$ each inhibitor compared to LPA-treated cells; one-way ANOVA with Bonferroni correction).

2018). Unfortunately, up to date, only a few selective antagonists for LPAR5 have been reported (Kozian et al., 2012, 2016; Murai et al., 2017). In a previous study, using one of those specific LPAR5 inhibitors (TCLPA5), we unraveled that the LPA/LPAR5 axis controls the inflammatory and migratory response in microglia cells (Plastira et al., 2016). In the present study, we analyzed the potency of two newly developed small molecule LPAR5 antagonists (AS2717638 and compound 3) to interfere with this LPA-induced pro-inflammatory response. AS2717638 was successfully used in preclinical rodent models of neuropathic pain where the inhibitor showed high potency,

selectivity, and CNS penetration with broad analgesic effects (Murai et al., 2017). Compound 3 is a diphenylpyrazole compound that was identified during a compound library screening approach (Kozian et al., 2016). Compound 3 is metabolically stable, has good absorption properties, and is bioavailable after oral administration in mice (Kozian et al., 2016). *In vitro*, compound 3 inhibits LPA-mediated activation (MCP-1 expression) of human mast cells or BV-2 microglia. However, and in contrast to AS2717638, compound 3 displays physicochemical properties that are predicted to have (according to Lipinski's "rule of five"; Lipinski et al., 2001) poor oral

absorption and/or distribution properties: the molecular weight is >500, logP is >5, and there are eight hydrogen-bond acceptors present in the compound (**Figure 1C**). On the other hand the polar surface area is <140 Å^2, which could compensate the high molecular weight (Veber et al., 2002) and mediate the good oral bioavailability observed in C57BL/6 mice (Kozian et al., 2016).

A first important observation from our *in vitro* study is that AS2717638 can regulate the BV-2 response to LPA at a 10-fold lower concentration compared to compound 3 (0.1 μM vs. 1 μM). Although both compounds have the potential to decrease cell viability, the concentrations inducing detrimental effects were far higher than the reported IC$_{50}$ values. These findings indicate an appropriate (*in vitro*) effect-to-toxicity window that is devoid of unspecific cellular responses. The inhibitory effects of the two LPAR5 antagonists were first assessed by analyzing their impact on the LPA-induced expression of different transcription factors. c-Jun is a component of AP-1 transcription factors and regulates the expression of many inflammatory and cytokine genes, which are involved in brain inflammation (Raivich, 2008). In addition, constitutive and inducible activation NF-kB in glial cells regulates inflammatory processes that exacerbate various diseases (Kaltschmidt and Kaltschmidt, 2009). Specifically in microglia, NF-kB regulated activation induced the release of pro-inflammatory cytokines and caused neurotoxicity (Block et al., 2007; Khasnavis et al., 2012; Yao et al., 2013; Frakes et al., 2014; Parisi et al., 2016). AS2717638 and compound 3 effectively inhibited phosphorylation of both c-Jun and p65 in LPA treated BV-2 cells at 8 and/or 24 h post-inhibitor addition indicating long-term regulation (**Figures 2A,B**). However, it should be noted that BV-2 cells used during the present study exhibit less pronounced induction of pro-inflammatory genes and lower cytokine secretion in response to LPS when compared to primary microglia (He et al., 2018), facts indicating potential limitations for the use of the BV-2 model.

In the CNS, STAT proteins are associated with development, hormone release, tumorigenesis, and inflammation (Nicolas et al., 2013). STATs are mediators of immunity and play important roles in inflammatory disease (O'Shea and Plenge, 2012). In brain tumors, STAT3 is highly upregulated (Gu et al., 2008; Chen et al., 2010). The role of STAT3 in brain inflammation is not entirely clear since both anti-inflammatory and pro-inflammatory mediators can activate it. In microglia, it was reported that the JAK2-STAT3 pathway induces pro-inflammatory responses (Huang et al., 2008; Yang et al., 2010). In contrast, the role of STAT1 is more clear-cut and usually promotes inflammation, expression of different cytokines, and production of NO and ROS (Delgado, 2003; Rezai-Zadeh et al., 2008; Herrera-Molina et al., 2012; Rauch et al., 2013). Different expression levels have been detected in glial cells (De-Fraja et al., 1998) and are associated with CNS pathological conditions such as brain inflammation (Hashioka et al., 2009), traumatic brain injury (Okada et al., 2006), and cerebral ischemia (Choi et al., 2005; Satriotomo et al., 2006). Both antagonists significantly decreased the activation of STAT3. Differences have been observed during STAT1 phosphorylation. Even though both, AS2717638 and compound 3 abrogated STAT1 activation

at 8 h, AS2717638 lost its inhibitory potential at the 24 h time point.

Microglia activation is accompanied by directed migration to the site of injury and subsequent release of cytokines, chemokines, NO, or ROS, which can have beneficial or detrimental effects on bystander cells (Ransohoff and Perry, 2009). The time-dependent expression profiles of cyto-/chemokines are specific for a pro- or anti-inflammatory microglia phenotype (Chhor et al., 2013). In response to LPA, an upregulated expression of IL-6, TNFα, IL-1β, CXCL10, CXCL2, and CCL5 was observed, in line with reports for LPS-activated primary murine microglia (Chhor et al., 2013). In addition, IL-1β, IL-6, TNFα, and the chemokines CCL5, and CXCL2 are implicated as regulators of the inflammatory response in (animal) models of TBI (Gyoneva and Ransohoff, 2015) where LPA concentrations are elevated (Crack et al., 2014). AS2717638 and compound 3 significantly decreased LPA-induced expression of those cytokines and chemokines, at least at one time point. Differences were observed for CXCL2, where AS2717638 had no statistically significant inhibitory effect. Both inhibitors abrogated the expression of COX2, CD40 and CD86 (pro-inflammatory markers). This is in line with earlier findings where we could demonstrate that TCLPA5 (an LPAR5 inhibitor) attenuates ERK1/2 and JNK activation, which both couple to COX-2 expression (Plastira et al., 2017). We can currently not offer an explanation for Arg1 upregulation in response to LPA (**Figure 4D**). In contrast to compound 3 only AS2717638 upregulated the anti-inflammatory markers Arg1 and CD206 (**Figures 4B,G**).

Microglia-induced neurotoxicity (Biber et al., 2014) is mediated by the constant production of pro-inflammatory cytokines and chemokines, NO (Liu et al., 2002), and ROS (Hsieh and Yang, 2013). An increase in oxidative stress might have detrimental effects (e.g., cell membrane damage, oxidative modification of lipids, covalent modification of intracellular proteins, or reduced antioxidant capacity of neurons) thereby promoting disease progression (Valko et al., 2007; Hsieh and Yang, 2013). During the present study, we found that supernatants collected from LPA plus AS2717638-treated BV-2 cells ameliorated cytotoxicity towards CATH.a neurons. Although compound 3 treatment showed a tendency for decreased neurotoxicity these effects were statistically not significant.

In conclusion, both LPAR5 antagonists are promising candidates to pharmacologically modulate the pro-inflammatory LPA/LPAR5 axis in microglia since AS2717638 and compound 3 abrogated phosphorylation of pro-inflammatory transcription factors and reduced secretion of inflammatory cytokines and chemokines. Our results point towards the possibility that LPAR5 antagonists might be useful pharmacological compounds to dampen the neuro-inflammatory response of microglia in CNS diseases that associate with aberrant LPA production.

DATA AVAILABILITY STATEMENT

All datasets generated for this study are included in the article/**Supplementary Material**.

AUTHOR CONTRIBUTIONS

FUNDING

SUPPLEMENTARY MATERIAL

The Supplementary Material for this article can be found online at: https://www.frontiersin.org/articles/10.3389/fncel.2019.005 31/full#supplementary-material.

REFERENCES

Amisten, S., Braun, O. O., Bengtsson, A., and Erlinge, D. (2008). Gene expression profiling for the identification of G-protein coupled receptors in human platelets. *Thromb. Res.* 122, 47–57. doi: 10.1016/j.thromres.2007.08.014

Aoki, J. (2004). Mechanisms of lysophosphatidic acid production. *Semin. Cell Dev. Biol.* 15, 477–489. doi: 10.1016/j.semcdb.2004.05.001

Aoki, J., Inoue, A., and Okudaira, S. (2008). Two pathways for lysophosphatidic acid production. *Biochim. Biophys, Acta* 1781, 513–518. doi: 10.1016/j.bbalip. 2008.06.005

Awada, R., Rondeau, P., Gres, S., Saulnier-Blache, J. S., Lefebvre d'Hellencourt, C., and Bourdon, E. (2012). Autotaxin protects microglial cells against oxidative stress. *Free Radic. Biol. Med.* 52, 516–526. doi: 10.1016/j.freeradbiomed.2011. 11.014

Awada, R., Saulnier-Blache, J. S., Gres, S., Bourdon, E., Rondeau, P., Parimisetty, A., et al. (2014). Autotaxin downregulates LPS-induced microglia activation and pro-inflammatory cytokines production. *J. Cell. Biochem.* 115, 2123–2132. doi: 10.1002/jcb.24889

Bernhart, E., Kollroser, M., Rechberger, G., Reicher, H., Heinemann, A., Schratl, P., et al. (2010). Lysophosphatidic acid receptor activation affects the C13NJ microglia cell line proteome leading to alterations in glycolysis, motility and cytoskeletal architecture. *Proteomics* 10, 141–158. doi: 10.1002/pmic. 200900195

Biber, K., Owens, T., and Boddeke, E. (2014). What is microglia neurotoxicity (Not)? *Glia* 62, 841–854. doi: 10.1002/glia.22654

Block, M. L., Zecca, L., and Hong, J. S. (2007). Microglia-mediated neurotoxicity: uncovering the molecular mechanisms. *Nat. Rev. Neurosci.* 8, 57–69. doi: 10.1038/nrn2038

Böttcher, C., Schlickeiser, S., Sneeboer, M. A. M., Kunkel, D., Knop, A., Paza, E., et al. (2019). Human microglia regional heterogeneity and phenotypes determined by multiplexed single-cell mass cytometry. *Nat. Neurosci.* 22, 78–90. doi: 10.1038/s41593-018-0290-2

Butovsky, O., and Weiner, H. L. (2018). Microglial signatures and their role in health and disease. *Nat. Rev. Neurosci.* 19, 622–635. doi: 10.1038/s41583-018-0057-5

Chen, F., Xu, Y., Luo, Y., Zheng, D., Song, Y., Yu, K., et al. (2010). Down-regulation of Stat3 decreases invasion activity and induces apoptosis of human glioma cells. *J. Mol. Neurosci.* 40, 353–359. doi: 10.1007/s12031-009-9323-3

Chhor, V., Le Charpentier, T., Lebon, S., Ore, M. V., Celador, I. L., Josserand, J., et al. (2013). Characterization of phenotype markers and neuronotoxic potential of polarised primary microglia *in vitro*. *Brain Behav. Immun.* 32, 70–85. doi: 10.1016/j.bbi.2013.02.005

Choi, S. H., Lee, D. Y., Kim, S. U., and Jin, B. K. (2005). Thrombin-induced oxidative stress contributes to the death of hippocampal neurons *in vivo*: role of microglial NADPH oxidase. *J. Neurosci.* 25, 4082–4090. doi: 10.1523/jneurosci. 4306-04.2005

Colonna, M., and Butovsky, O. (2017). Microglia function in the central nervous system during health and neurodegeneration. *Annu. Rev. Immunol.* 35, 441–468. doi: 10.1146/annurev-immunol-051116-052358

Crack, P. J., Zhang, M., Morganti-Kossmann, M. C., Morris, A. J., Wojciak, J. M., Fleming, J. K., et al. (2014). Anti-lysophosphatidic acid antibodies improve traumatic brain injury outcomes. *J. Neuroinflammation* 11:37. doi: 10.1186/1742-2094-11-37

Daina, A., Michielin, O., and Zoete, V. (2017). SwissADME: a free web tool to evaluate pharmacokinetics, drug-likeness and medicinal chemistry friendliness of small molecules. *Sci. Rep.* 7:42717. doi: 10.1038/srep42717

De-Fraja, C., Conti, L., Magrassi, L., Govoni, S., and Cattaneo, E. (1998). Members of the JAK/STAT proteins are expressed and regulated during development in the mammalian forebrain. *J. Neurosci. Res.* 54, 320–330. doi: 10.1002/(sici)1097-4547(19981101)54:3<320::aid-jnr3>3.0.co;2-r

Delgado, M. (2003). Inhibition of interferon (IFN) γ-induced Jak-STAT1 activation in microglia by vasoactive intestinal peptide: inhibitory effect on CD40, IFN-induced protein-10, and inducible nitric-oxide synthase expression. *J. Biol. Chem.* 278, 27620–27629. doi: 10.1074/jbc.M303 199200

Du, L., Zhang, Y., Chen, Y., Zhu, J., Yang, Y., and Zhang, H.-L. (2016). Role of microglia in neurological disorders and their potentials as a therapeutic target. *Mol. Neurobiol.* 54, 7567–7584. doi: 10.1007/s12035-016-0245-0

Eisenried, A., Meidahl, A. C. N., Klukinov, M., Tzabazis, A. Z., Sabbadini, R. A., Clark, J. D., et al. (2017). Nervous system delivery of antilysophosphatidic acid antibody by nasal application attenuates mechanical allodynia after traumatic brain injury in rats. *Pain* 158, 2181–2188. doi: 10.1097/j.pain. 0000000000001019

Frakes, A. E., Ferraiuolo, L., Haidet-Phillips, A. M., Schmelzer, L., Braun, L., Miranda, C. J., et al. (2014). Microglia induce motor neuron death *via* the classical NF-κB pathway in amyotrophic lateral sclerosis. *Neuron* 81, 1009–1023. doi: 10.1016/j.neuron.2014.01.013

Garaschuk, O., and Verkhratsky, A. (2019). Physiology of microglia. *Methods Mol. Biol.* 2034, 27–40. doi: 10.1007/978-1-4939-9658-2_3

Ginhoux, F., and Prinz, M. (2015). Origin of microglia: current concepts and past controversies. *Cold Spring Harb. Perspect. Biol.* 7:a020537. doi: 10.1101/cshperspect.a020537

Ginhoux, F., Greter, M., Leboeuf, M., Nandi, S., See, P., Gokhan, S., et al. (2010). Fate mapping analysis reveals that adult microglia derive from primitive macrophages. *Science* 330, 841–845. doi: 10.1126/science.1194637

Grabert, K., Michoel, T., Karavolos, M. H., Clohisey, S., Baillie, J. K., Stevens, M. P., et al. (2016). Microglial brain region-dependent diversity and selective regional sensitivities to aging. *Nat. Neurosci.* 19, 504–516. doi: 10.1038/nn.4222

Gu, J., Li, G., Sun, T., Su, Y., Zhang, X., Shen, J., et al. (2008). Blockage of the STAT3 signaling pathway with a decoy oligonucleotide suppresses growth of human malignant glioma cells. *J. Neurooncol.* 89, 9–17. doi: 10.1007/s11060-008-9590-9

Guneykaya, D., Ivanov, A., Hernandez, D. P., Haage, V., Wojtas, B., Meyer, N., et al. (2018). Transcriptional and translational differences of microglia from male and female brains. *Cell Rep.* 24, 2773.e6–2783.e6. doi: 10.1016/j.celrep. 2018.08.001

Gyoneva, S., and Ransohoff, R. M. (2015). Inflammatory reaction after traumatic brain injury: therapeutic potential of targeting cell-cell communication by

chemokines. *Trends Pharmacol. Sci.* 36, 471–480. doi: 10.1016/j.tips.2015.04.003

Hammond, T. R., Dufort, C., Dissing-Olesen, L., Giera, S., Young, A., Wysoker, A., et al. (2019). Single-Cell RNA sequencing of microglia throughout the mouse lifespan and in the injured brain reveals complex cell-state changes. *Immunity* 50, 253.e6–271.e6. doi: 10.1016/j.immuni.2018.11.004

Hammond, T. R., Robinton, D., and Stevens, B. (2018). Microglia and the brain: complementary partners in development and disease. *Annu. Rev. Cell Dev. Biol.* 34, 523–544. doi: 10.1146/annurev-cellbio-100616-060509

Hashioka, S., Klegeris, A., Schwab, C., and McGeer, P. L. (2009). Interferon-gamma-dependent cytotoxic activation of human astrocytes and astrocytoma cells. *Neurobiol. Aging.* 30, 1924–1935. doi: 10.1016/j.neurobiolaging.2008.02.019

He, Y., Yao, X., Taylor, N., Bai, Y., Lovenberg, T., and Bhattacharya, A. (2018). RNA sequencing analysis reveals quiescent microglia isolation methods from postnatal mouse brains and limitations of BV2 cells. *J. Neuroinflammation* 15:153. doi: 10.1186/s12974-018-1195-4

Herr, D. R., Ong, J. H., and Ong, W. Y. (2018). Potential therapeutic applications for inhibitors of autotaxin, a bioactive lipid-producing lysophospholipase D, in disorders affecting the nervous system. *ACS Chem. Neurosci.* 9, 398–400. doi: 10.1021/acschemneuro.8b00057

Herrera-Molina, R., Flores, B., Orellana, J. A., and von Bernhardi, R. (2012). Modulation of interferon-γ-induced glial cell activation by transforming growth factor β1: a role for STAT1 and MAPK pathways. *J. Neurochem.* 123, 113–123. doi: 10.1111/j.1471-4159.2012.07887.x

Hickman, S. E., Kingery, N. D., Ohsumi, T. K., Borowsky, M. L., Wang, L. C., Means, T. K., et al. (2013). The microglial sensome revealed by direct RNA sequencing. *Nat. Neurosci.* 16, 1896–1905. doi: 10.1038/nn.3554

Hickman, S., Izzy, S., Sen, P., Morsett, L., and El Khoury, J. (2018). Microglia in neurodegeneration. *Nat. Neurosci.* 21, 1359–1369. doi: 10.1038/s41593-018-0242-x

Hsieh, H. L., and Yang, C. M. (2013). Role of redox signaling in neuroinflammation and neurodegenerative diseases. *Biomed. Res. Int.* 2013:484613. doi: 10.1155/2013/484613

Huang, C., Ma, R., Sun, S., Wei, G., Fang, Y., Liu, R., et al. (2008). JAK2-STAT3 signaling pathway mediates thrombin-induced proinflammatory actions of microglia *in vitro. J. Neuroimmunol.* 204, 118–125. doi: 10.1016/j.jneuroim.2008.07.004

Kaltschmidt, B., and Kaltschmidt, C. (2009). NF-κB in the nervous system. *Cold Spring Harb. Perspect. Biol.* 1:a001271. doi: 10.1101/cshperspect.a001271

Kano, K., Arima, N., Ohgami, M., and Aoki, J. (2008). LPA and its analogs-attractive tools for elucidation of LPA biology and drug development. *Curr. Med. Chem.* 15, 2122–2131. doi: 10.2174/092986708785747562

Kawamoto, Y., Seo, R., Murai, N., Hiyama, H., and Oka, H. (2018). Identification of potent lysophosphatidic acid receptor 5 (LPA5) antagonists as potential analgesic agents. *Bioorg. Med. Chem.* 26, 257–265. doi: 10.1016/j.bmc.2017.11.038

Khasnavis, S., Jana, A., Roy, A., Mazumder, M., Bhushan, B., Wood, T., et al. (2012). Suppression of nuclear factor-κB activation and inflammation in microglia by physically modified saline. *J. Biol. Chem.* 287, 29529–29542. doi: 10.1074/jbc.M111.338012

Kotarsky, K., Boketoft, A., Bristulf, J., Nilsson, N. E., Norberg, A., Hansson, S., et al. (2006). Lysophosphatidic acid binds to and activates GPR92, a G protein-coupled receptor highly expressed in gastrointestinal lymphocytes. *J. Pharmacol. Exp. Ther.* 318, 619–628. doi: 10.1124/jpet.105.098848

Kozian, D. H., Evers, A., Florian, P., Wonerow, P., Joho, S., and Nazare, M. (2012). Selective non-lipid modulator of LPA5 activity in human platelets. *Bioorg. Med. Chem. Lett.* 22, 5239–5243. doi: 10.1016/j.bmcl.2012.06.057

Kozian, D. H., von Haeften, E., Joho, S., Czechtizky, W., Anumala, U. R., Roux, P., et al. (2016). Modulation of hexadecyl-LPA-mediated activation of mast cells and microglia by a chemical probe for LPA5. *Chembiochem* 17, 861–865. doi: 10.1002/cbic.201500559

Lee, C. W., Rivera, R., Gardell, S., Dubin, A. E., and Chun, J. (2006). GPR92 as a new G12/13- and Gq-coupled lysophosphatidic acid receptor that increases cAMP, LPA5. *J. Biol. Chem.* 281, 23589–23597. doi: 10.1074/jbc.m603670200

Lin, M. E., Rivera, R. R., and Chun, J. (2012). Targeted deletion of LPA5 identifies novel roles for lysophosphatidic acid signaling in development of neuropathic pain. *J. Biol. Chem.* 287, 17608–17617. doi: 10.1074/jbc.m111.330183

Lipinski, C. A., Lombardo, F., Dominy, B. W., and Feeney, P. J. (2001). Experimental and computational approaches to estimate solubility and permeability in drug discovery and development settings. *Adv. Drug Deliv. Rev.* 46, 3–26. doi: 10.1016/s0169-409x(00)00129-0

Liu, B., Gao, H. M., Wang, J. Y., Jeohn, G. H., Cooper, C. L., and Hong, J. S. (2002). Role of nitric oxide in inflammation-mediated neurodegeneration. *Ann. N. Y. Acad. Sci.* 962, 318–331. doi: 10.1111/j.1749-6632.2002.tb04077.x

Lundequist, A., and Boyce, J. A. (2011). LPA5 is abundantly expressed by human mast cells and important for lysophosphatidic acid induced MIP-1β release. *PLoS One* 6:e18192. doi: 10.1371/journal.pone.0018192

Ma, L., Uchida, H., Nagai, J., Inoue, M., Aoki, J., and Ueda, H. (2010). Evidence for *de novo* synthesis of lysophosphatidic acid in the spinal cord through phospholipase A2 and autotaxin in nerve injury-induced neuropathic pain. *J. Pharmacol. Exp. Ther.* 333, 540–546. doi: 10.1124/jpet.109.164830

Masuda, T., Sankowski, R., Staszewski, O., Bottcher, C., Amann, L., and Sagar, et al. (2019). Spatial and temporal heterogeneity of mouse and human microglia at single-cell resolution. *Nature* 566, 388–392. doi: 10.1038/s41586-019-0924-x

Matralis, A. N., Afantitis, A., and Aidinis, V. (2019). Development and therapeutic potential of autotaxin small molecule inhibitors: from bench to advanced clinical trials. *Med. Res. Rev.* 39, 976–1013. doi: 10.1002/med.21551

Möller, T., Contos, J. J., Musante, D. B., Chun, J., and Ransom, B. R. (2001). Expression and function of lysophosphatidic acid receptors in cultured rodent microglial cells. *J. Biol. Chem.* 276, 25946–25952. doi: 10.1074/jbc.m102691200

Mukherjee, S., Klaus, C., Pricop-Jeckstadt, M., Miller, J. A., and Struebing, F. L. (2019). A microglial signature directing human aging and neurodegeneration-related gene networks. *Front. Neurosci.* 13:2. doi: 10.3389/fnins.2019.00002

Murai, N., Hiyama, H., Kiso, T., Sekizawa, T., Watabiki, T., Oka, H., et al. (2017). Analgesic effects of novel lysophosphatidic acid receptor 5 antagonist AS2717638 in rodents. *Neuropharmacology* 126, 97–107. doi: 10.1016/j.neuropharm.2017.08.032

Nicolas, C. S., Amici, M., Bortolotto, Z. A., Doherty, A., Csaba, Z., Fafouri, A., et al. (2013). The role of JAK-STAT signaling within the CNS. *JAKSTAT* 2:e22925. doi: 10.4161/jkst.22925

Nimmerjahn, A., Kirchhoff, F., and Helmchen, F. (2005). Resting microglial cells are highly dynamic surveillants of brain parenchyma *in vivo. Science* 308, 1314–1318. doi: 10.1126/science.1110647

Norris, G. T., and Kipnis, J. (2019). Immune cells and CNS physiology: microglia and beyond. *J. Exp. Med.* 216, 60–70. doi: 10.1084/jem.20180199

Ohuchi, H., Hamada, A., Matsuda, H., Takagi, A., Tanaka, M., Aoki, J., et al. (2008). Expression patterns of the lysophospholipid receptor genes during mouse early development. *Dev. Dyn.* 237, 3280–3294. doi: 10.1002/dvdy.21736

Okada, S., Nakamura, M., Katoh, H., Miyao, T., Shimazaki, T., Ishii, K., et al. (2006). Conditional ablation of Stat3 or Socs3 discloses a dual role for reactive astrocytes after spinal cord injury. *Nat. Med.* 12, 829–834. doi: 10.1038/nm1425

O'Shea, J. J., and Plenge, R. (2012). JAK and STAT signaling molecules in immunoregulation and immune-mediated disease. *Immunity* 36, 542–550. doi: 10.1016/j.immuni.2012.03.014

Parisi, C., Napoli, G., Amadio, S., Spalloni, A., Apolloni, S., Longone, P., et al. (2016). MicroRNA-125b regulates microglia activation and motor neuron death in ALS. *Cell Death Differ.* 23, 531–541. doi: 10.1038/cdd.2015.153

Plastira, I., Bernhart, E., Goeritzer, M., DeVaney, T., Reicher, H., Hammer, A., et al. (2017). Lysophosphatidic acid *via* LPA-receptor 5/protein kinase D-dependent pathways induces a motile and pro-inflammatory microglial phenotype. *J. Neuroinflammation* 14:253. doi: 10.1186/s12974-017-1024-1

Plastira, I., Bernhart, E., Goeritzer, M., Reicher, H., Kumble, V. B., Kogelnik, N., et al. (2016). 1-Oleyl-lysophosphatidic acid (LPA) promotes polarization of BV-2 and primary murine microglia towards an M1-like phenotype. *J. Neuroinflammation* 13:205. doi: 10.1186/s12974-016-0701-9

Raivich, G. (2008). c-Jun expression, activation and function in neural cell death, inflammation and repair. *J. Neurochem.* 107, 898–906. doi: 10.1111/j.1471-4159.2008.05684.x

Ramesh, S., Govindarajulu, M., Suppiramaniam, V., Moore, T., and Dhanasekaran, M. (2018). Autotaxin-lysophosphatidic acid signaling in Alzheimer's disease. *Int. J. Mol. Sci.* 19:1827. doi: 10.3390/ijms19071827

Ransohoff, R. M., and Brown, M. A. (2012). Innate immunity in the central nervous system. *J. Clin. Invest.* 122, 1164–1171. doi: 10.1172/JCI58644

Ransohoff, R. M., and Cardona, A. E. (2010). The myeloid cells of the central nervous system parenchyma. *Nature* 468, 253–262. doi: 10.1038/nature09615

Ransohoff, R. M., and Perry, V. H. (2009). Microglial physiology: unique stimuli, specialized responses. *Annu. Rev. Immunol.* 27, 119–145. doi: 10.1146/annurev.immunol.021908.132528

Rauch, I., Müller, M., and Decker, T. (2013). The regulation of inflammation by interferons and their STATs. *JAKSTAT* 2:e23820. doi: 10.4161/jkst.23820

Rezai-Zadeh, K., Ehrhart, J., Bai, Y., Sanberg, P. R., Bickford, P., Tan, J., et al. (2008). Apigenin and luteolin modulate microglial activation *via* inhibition of STAT1-induced CD40 expression. *J. Neuroinflammation* 5:41. doi: 10.1186/1742-2094-5-41

Salter, M. W., and Stevens, B. (2017). Microglia emerge as central players in brain disease. *Nat. Med.* 23, 1018–1027. doi: 10.1038/nm.4397

Santos-Nogueira, E., López-Serrano, C., Hernández, J., Lago, N., Astudillo, A. M., Balsinde, J., et al. (2015). Activation of lysophosphatidic acid receptor type 1 contributes to pathophysiology of spinal cord injury. *J. Neurosci.* 35, 10224–10235. doi: 10.1523/JNEUROSCI.4703-14.2015

Satriotomo, I., Bowen, K. K., and Vemuganti, R. (2006). JAK2 and STAT3 activation contributes to neuronal damage following transient focal cerebral ischemia. *J. Neurochem.* 98, 1353–1368. doi: 10.1111/j.1471-4159.2006.04051.x

Savaskan, N. E., Rocha, L., Kotter, M. R., Baer, A., Lubec, G., van Meeteren, L. A., et al. (2007). Autotaxin (NPP-2) in the brain: cell type-specific expression and regulation during development and after neurotrauma. *Cell Mol. Life Sci.* 64, 230–243. doi: 10.1007/s00018-006-6412-0

Schilling, T., Repp, H., Richter, H., Koschinski, A., Heinemann, U., Dreyer, F., et al. (2002). Lysophospholipids induce membrane hyperpolarization in microglia by activation of IKCa1 Ca^{2+}-dependent K^+ channels. *Neuroscience* 109, 827–835. doi: 10.1016/s0306-4522(01)00534-6

Schilling, T., Stock, C., Schwab, A., and Eder, C. (2004). Functional importance of Ca2+-activated K+ channels for lysophosphatidic acid-induced microglial migration. *Eur. J. Neurosci.* 19, 1469–1474. doi: 10.1111/j.1460-9568.2004.03265.x

Smolders, S. M., Kessels, S., Vangansewinkel, T., Rigo, J. M., Legendre, P., and Brone, B. (2019). Microglia: brain cells on the move. *Prog. Neurobiol.* 178:101612. doi: 10.1016/j.pneurobio.2019.04.001

Song, W. M., and Colonna, M. (2018). The identity and function of microglia in neurodegeneration. *Nat. Immunol.* 19, 1048–1058. doi: 10.1038/s41590-018-0212-1

Sun, L., Wu, Z., Hayashi, Y., Peters, C., Tsuda, M., Inoue, K., et al. (2012). Microglial cathepsin B contributes to the initiation of peripheral inflammation-induced chronic pain. *J. Neurosci.* 32, 11330–11342. doi: 10.1523/JNEUROSCI.0677-12.2012

Tabuchi, S. (2015). The autotaxin-lysophosphatidic acid-lysophosphatidic acid receptor cascade: proposal of a novel potential therapeutic target for treating glioblastoma multiforme. *Lipids Health Dis.* 14:56. doi: 10.1186/s12944-015-0059-5

Tang, Y., and Le, W. (2016). Differential roles of M1 and M2 microglia in neurodegenerative diseases. *Mol. Neurobiol.* 53, 1181–1194. doi: 10.1007/s12035-014-9070-5

Tay, T. L., Sagar, Dautzenberg, J., Grün, D., and Prinz, M. (2018). Unique microglia recovery population revealed by single-cell RNAseq following neurodegeneration. *Acta Neuropathol. Commun.* 6:87. doi: 10.1186/s40478-018-0584-3

Tigyi, G., Hong, L., Yakubu, M., Parfenova, H., Shibata, M., and Leffler, C. W. (1995). Lysophosphatidic acid alters cerebrovascular reactivity in piglets. *Am. J. Physiol.* 268, H2048–S2055. doi: 10.1152/ajpheart.1995.268.5.H2048

Tsukahara, R., Yamamoto, S., Yoshikawa, K., Gotoh, M., Tsukahara, T., Neyama, H., et al. (2018). LPA5 signaling is involved in multiple sclerosis-mediated neuropathic pain in the cuprizone mouse model. *J. Pharmacol. Sci.* 136, 93–96. doi: 10.1016/j.jphs.2018.01.001

Ueda, H., Matsunaga, H., Olaposi, O. I., and Nagai, J. (2013). Lysophosphatidic acid: chemical signature of neuropathic pain. *Biochim. Biophys. Acta* 1831, 61–73. doi: 10.1016/j.bbalip.2012.08.014

Umemura, K., Yamashita, N., Yu, X., Arima, K., Asada, T., Makifuchi, T., et al. (2006). Autotaxin expression is enhanced in frontal cortex of Alzheimer-type dementia patients. *Neurosci. Lett.* 400, 97–100. doi: 10.1016/j.neulet.2006.02.008

Valko, M., Leibfritz, D., Moncol, J., Cronin, M. T., Mazur, M., and Telser, J. (2007). Free radicals and antioxidants in normal physiological functions and human disease. *Int. J. Biochem. Cell Biol.* 39, 44–84. doi: 10.1016/j.biocel.2006.07.001

Veber, D. F., Johnson, S. R., Cheng, H. Y., Smith, B. R., Ward, K. W., and Kopple, K. D. (2002). Molecular properties that influence the oral bioavailability of drug candidates. *J. Med. Chem.* 45, 2615–2623. doi: 10.1021/jm020017n

Vodicka, P., Mo, S., Tousley, A., Green, K. M., Sapp, E., Iuliano, M., et al. (2015). Mass spectrometry analysis of wild-type and knock-in Q140/Q140 Huntington's disease mouse brains reveals changes in glycerophospholipids including alterations in phosphatidic acid and lyso-phosphatidic acid. *J. Huntingtons Dis.* 4, 187–201. doi: 10.3233/JHD-150149

Waltl, S., Patankar, J. V., Fauler, G., Nusshold, C., Ullen, A., Eibinger, G., et al. (2013). 25-Hydroxycholesterol regulates cholesterol homeostasis in the murine CATH.a neuronal cell line. *Neurosci. Lett.* 539, 16–21. doi: 10.1016/j.neulet.2013.01.014

Wolf, S. A., Boddeke, H. W., and Kettenmann, H. (2017). Microglia in physiology and disease. *Annu. Rev. Physiol.* 79, 619–643. doi: 10.1146/annurev-physiol-022516-034406

Yang, X., He, G., Hao, Y., Chen, C., Li, M., Wang, Y., et al. (2010). The role of the JAK2-STAT3 pathway in pro-inflammatory responses of EMF-stimulated N9 microglial cells. *J. Neuroinflammation* 7:54. doi: 10.1186/1742-2094-7-54

Yang, X.-Y., Zhao, E. Y., Zhuang, W.-X., Sun, F.-X., Han, H.-L., Han, H.-R., et al. (2015). LPA signaling is required for dopaminergic neuron development and is reduced through low expression of the LPA1 receptor in a 6-OHDA lesion model of Parkinson's disease. *Neurol. Sci.* 36, 2027–2033. doi: 10.1007/s10072-015-2295-x

Yao, L., Kan, E. M., Kaur, C., Dheen, S. T., Hao, A., Lu, J., et al. (2013). Notch-1 signaling regulates microglia activation *via* NF-κB pathway after hypoxic exposure *in vivo* and *in vitro*. *PLoS One* 8:e78439. doi: 10.1371/journal.pone.0078439

Yung, Y. C., Mutoh, T., Lin, M. E., Noguchi, K., Rivera, R. R., Choi, J. W., et al. (2011). Lysophosphatidic acid signaling may initiate fetal hydrocephalus. *Sci. Transl. Med.* 3:99ra87. doi: 10.1126/scitranslmed.3002095

Yung, Y. C., Stoddard, N. C., and Chun, J. (2014). LPA receptor signaling: pharmacology, physiology and pathophysiology. *J. Lipid Res.* 55, 1192–1214. doi: 10.1194/jlr.R046458